Available at www.ElsevierComputerScience.com
POWERED BY SCIENCE DIRECT®

Signal Processing ▮ (▮▮▮▮) ▮▮▮–▮▮▮

SIGNAL PROCESSING

www.elsevier.com/locate/sigpro

Data-aided frame timing acquisition for fractal modulation in an AWGN channel

Chih-Ming Fu[a], Wen-Liang Hwang[b,*], Chung-Lin Huang[a]

[a]Department of Electrical Engineering, National Tsing Hua University, Taiwan
[b]Institute of Information Science, Academia Sinica, Nankang, Taipei, Taiwan

Received 1 March 2004; received in revised form 2 February 2005

Abstract

We propose a frame timing acquisition algorithm for fractal modulation in additive white Gaussian noise (AWGN) channels. Our algorithm exclusively uses the data redundancy inherent in fractal modulation to locate the start time of all the sub-bands (start-of-frame). The acquisition functions are derived using the maximum-likelihood method and the start-of-frame that maximizes the function attained by a serial search algorithm. Monte-Carlo simulations are conducted to evaluate the mean acquisition time of our algorithm.

Keywords: Fractals; Synchronization; Wavelet transforms

1. Introduction

In studies of fractal modulation, it is assumed that the start-of-frame of a fractal modulation is known, but a technique to detect it has heretofore not been developed. A fractal modulation modulates the same data into different time-frequency cells. The diversity property results in the reliable transmission of data in a channel whose duration and bandwidth are both unknown to the transmitter [1,2]. This property has been used to study channel estimation, equalization design, and data transmission in a fading environment [3–5]. These applications assume that the start-of-frame of a fractal modulation is known. When the start-of-frame is correctly detected, the time-frequency cells containing the same data can be identified, and the diversity property can be applied.

This frame synchronization, however, cannot be obtained by a wavelet modulation synchronization algorithm. Although such an algorithm can be used to obtain the symbol timing of sub-bands, it cannot be used to find time-frequency cells that contain the same data [6,7]. We, therefore, need to develop a new frame timing recovery method for detection of the start-of-frame instant of fractal modulation.

*Corresponding author.
E-mail address: whwang@iis.sinica.edu.tw (W.-L. Hwang).

0165-1684/$ - see front matter
doi:10.1016/j.sigpro.2005.05.010

We assume that baseband transmission is used and that the time domain clock error is the major factor that degrades the performance of a receiver. We propose a data-aided maximum likelihood approach to derive a data-aided frame timing acquisition function for a fractal modulated signal that exclusively uses the data redundancy inherent in fractal modulation. A series search approach is proposed to avoid calculating the derivative of the irregular likelihood function and finding the zero of the derivative.

In Section 2, we review fractal modulation and demodulation. In Section 3, we derive a frame timing acquisition function using a maximum likelihood approach; a serial search algorithm is introduced in Section 3.1. Simulation results of the acquisition performance are shown in Section 4. Finally, in Section 5, we present our conclusion and indicate the direction of future work to improve frame timing acquisition.

2. Fractal modulation and demodulation

An orthogonal wavelet is the basic signal waveform of fractal modulation. In an orthogonal wavelet transform, basis functions are all dilations and translations of a single function called a mother wavelet $\psi(t)$. An orthogonal wavelet transformation of a signal $x(t)$, with the wavelet $\psi(x)$, is described in terms of synthesis and analysis equations in which the inverse wavelet transform is

$$x(t) = \sum_m \sum_n x_{m,n}\psi_{m,n}(t), \tag{1}$$

and the wavelet transform is

$$x_{m,n} = \int x(t)\psi_{m,n}(t)\,\mathrm{d}t, \tag{2}$$

where

$$\psi_{m,n}(t) = 2^{m/2}\psi(2^m t - n), \tag{3}$$

and m and n are the dilation and translation indices. The inner product between $\psi_{m,n}(t)$ and $\psi_{p,q}(t)$ satisfies the orthogonal property

$$\langle\psi_{m,n}(t), \psi_{p,q}(t)\rangle = \int \psi_{m,n}(t)\psi_{p,q}(t)\,\mathrm{d}t = \delta_{m,p}\delta_{n,q}. \tag{4}$$

A deterministic self-similarity signal $s(t)$ satisfies the deterministic scale-invariance property

$$s(t) = a^{-H}s(at) \tag{5}$$

for all $a > 0$. We only consider the waveforms that satisfy the dyadic self-similar property

$$s(t) = 2^{-kH}s(2^k t) \tag{6}$$

for all integer k, and hereafter refer to them simply as self-similar signals. The wavelet transform of $s(t)$ yields a set of re-normalization coefficients $\{s_{m,n}\}$ in which $s_{m,n} = \beta^{-m/2}s_{0,n}$ and $\beta = 2^{2H+1}$ are found.

From a discrete sequence $\{d_n\}$, fractal modulation produces a self-similar signal by performing the inverse wavelet transform

$$s(t) = \sum_m \sum_n \beta^{-m/2}\, d_n\psi_{m,n}(t). \tag{7}$$

If $\{d_n\}$ has finite length L, then the finite length message is extended as a periodic sequence $\{d_{(n \bmod L)}\}$ and, as a result, generates the transmission waveform

$$s(t) = \sum_n d_{(n \bmod L)} \sum_m \beta^{-m/2}\psi_{m,n}(t). \tag{8}$$

Fig. 1shows a finite length data vector in a time and frequency plane in which many time frequency cells carry the same data.

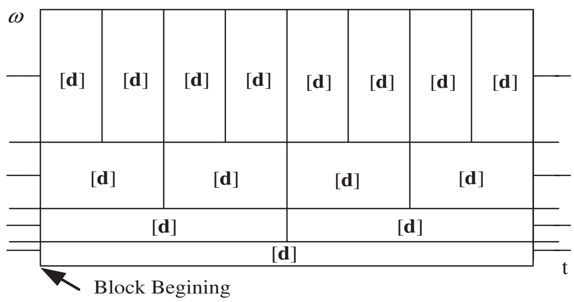

Fig. 1. A frame of a transmitted signal with a finite-length data vector. The bottom row corresponds to the sub-band $m = 0$. The data vector is transmitted repeatedly in a sub-band with $m > 0$.

We use *fractal group* to refer to a collection of time-frequency cells containing the same information $d_{(n \bmod L)}$ in a time frequency plane. For data length L, we have a total of L fractal groups. The time-frequency indices of fractal group G_i are $\{(m,n)|m = 0, 1, \ldots, M-1$ and $(n \bmod L) = i\}$, where m and n are scale and time indices, respectively. Eq. (8) can be rewritten as a modulation of the finite length data $\{d_{(n \bmod L)}\}$ using a modulation waveform $\varphi_i(t)$ (called a modulation fractal basis hereafter) $\varphi_i(t)$

$$s(t) = \sum_{i=0}^{L-1} d_i \sum_{(m,n)\in G_i} \beta^{-m/2}\psi_{m,n}(t) = \sum_{i=0}^{L-1} d_i\varphi_i(t), \tag{9}$$

where

$$\varphi_i(t) = \sum_{(m,n)\in G_i} \beta^{-m/2}\psi_{m,n}(t) \tag{10}$$

is a weighted summation of wavelets with time-frequency indices containing d_i. For demodulation, we use the demodulation waveform $\bar{\varphi}_i(t)$ (also called demodulation fractal basis), which is defined as

$$\bar{\varphi}_i(t) = \sum_{(m,n)\in G_i} \beta^{m/2}\psi_{m,n}(t). \tag{11}$$

The modulation and demodulation fractal bases are linear combinations of the wavelet basis but have different weighting functions. They are self-similar and satisfy the orthogonal properties

$$\int \varphi_i(t)\bar{\varphi}_k(t)\,\mathrm{d}t = \eta_i\delta_{i,k}, \tag{12}$$

$$\int \varphi_i(t)\varphi_k(t)\,\mathrm{d}t = \eta_i^m\delta_{i,k}, \tag{13}$$

$$\int \bar{\varphi}_i(t)\bar{\varphi}_k(t)\,\mathrm{d}t = \eta_i^d\delta_{i,k}, \tag{14}$$

where η_i, η_i^m, and η_i^d are, respectively, $\sum_{(m,n)\in G_i} 1$, $\sum_{(m,n)\in G_i} \beta^{-m}$, and $\sum_{(m,n)\in G_i} \beta^{m}$. We hereafter focus on fractal groups that have the same number of elements. In such cases, if there are M sub-bands, we have $\eta = \eta_i = 2^M - 1$, $\eta_m = \eta_i^m = (1-(2\beta^{-1})^M)/(1-2\beta^{-1})$, and $\eta_d = \eta_i^d = (1-(2\beta)^M)/(1-2\beta)$, where η is the redundancy factor. Furthermore, if $\beta = 1$, then $\eta = \eta_d = \eta_m$.

3. Frame timing acquisition in an AWGN channel

We use $\mathbf{d} = [d_0, d_1, \ldots, d_{L-1}]^{\mathrm{T}}$ as the information vector with independent $d_i \in \{\sqrt{E_b}, -\sqrt{E_b}\}$. A received waveform with transmission delay τ can be written as

$$r(t;\tau) = s(t-\tau) + w(t). \tag{15}$$

Suppose that $w(t)$ in Eq. (15) is a white Gaussian noise with a zero mean and variance σ^2. If a demodulation fractal basis $\bar{\varphi}_i(t)$ is used to extract the information bit d_i by projecting the received signal $r(t)$ onto the basis, we have

$$r_i(\hat{\tau};\tau) = \int r(t;\tau)\bar{\varphi}_i(t-\hat{\tau})\,\mathrm{d}t \tag{16}$$

$$= s_i(\hat{\tau}-\tau) + w_i(\hat{\tau}), \tag{17}$$

where

$$s_i(\hat{\tau}-\tau) = \int s(t-\tau)\bar{\varphi}_i(t-\hat{\tau})\,\mathrm{d}t, \tag{18}$$

$$w_i(\hat{\tau}) = \int w(t)\bar{\varphi}_i(t-\hat{\tau})\,\mathrm{d}t. \tag{19}$$

$w_i(\hat{\tau})$ is again a zero mean uncorrelated Gaussian noise and

$$E[w_i(\hat{\tau})] = \int E[w(t)]\bar{\varphi}_i(t-\hat{\tau})\,\mathrm{d}t = 0 \tag{20}$$

$$E[w_i(\hat{\tau})w_k(\hat{\tau})]$$

$$= \int\int E[w(t)w(t')]\bar{\varphi}_i(t-\hat{\tau})\bar{\varphi}_k(t'-\hat{\tau})\,\mathrm{d}t\,\mathrm{d}t' \tag{21}$$

$$= \int \sigma^2\bar{\varphi}_i(t-\hat{\tau})\bar{\varphi}_k(t-\hat{\tau})\,\mathrm{d}t \tag{22}$$

$$= \eta_d\sigma^2\delta_{i,k}. \tag{23}$$

Therefore, $r_i(\hat{\tau};\tau)$ is an independent random variable for each i, and the joint pdf of the vector $\mathbf{r} = [r_0(\hat{\tau};\tau)r_1(\hat{\tau};\tau)\cdots r_{L-1}(\hat{\tau};\tau)]^{\mathrm{T}}$ becomes

$$p(\mathbf{r}|\hat{\tau}-\tau,\mathbf{d})$$

$$= \left(\frac{1}{\sqrt{2\pi\eta_d}\sigma}\right)^L \exp\left\{-\frac{1}{2\eta_d\sigma^2} \times \sum_{i=0}^{L-1}[r_i(\hat{\tau};\tau) - s_i(\hat{\tau}-\tau)]^2\right\}. \tag{24}$$

Omitting all constant terms, we obtain the log-likelihood function

$$\Lambda_L(\hat{\tau}) = \sum_{i=0}^{L-1} [r_i(\hat{\tau};\tau) - s_i(\hat{\tau}-\tau)]^2. \tag{25}$$

When the frame timing is acquired, as in the case where $\hat{\tau} = \tau$, we have $s_i(0) = \eta d_i$. Thus, we use ηd_i to approximate $s_i(\hat{\tau}-\tau)$ in the above equation, and the log-likelihood function becomes

$$\Lambda_L(\hat{\tau}) \approx \sum_{i=0}^{L-1} [r_i(\hat{\tau};\tau) - \eta d_i]^2 \tag{26}$$

$$= \sum_{i=0}^{L-1} r_i(\hat{\tau};\tau)^2 - 2\eta \sum_{i=0}^{L-1} r_i(\hat{\tau};\tau) d_i + \sum_{i=0}^{L-1} \eta^2 d_i^2. \tag{27}$$

The first term in Eq. (27) can be approximated as the power of the received signal. The last term of Eq. (27) is a constant, since $\sum_{i=0}^{L-1} \eta^2 d_i^2 = L\eta^2 E_b$. After ignoring these two terms in Eq. (27), and dividing the result by the total number of cells in a block, $L\eta$, the frame timing can be obtained by finding the maximum value of the following acquisition function:

$$\Lambda_{\text{acq}}(\hat{\tau};\tau) = \frac{1}{L\eta} \sum_{i=0}^{L-1} r_i(\hat{\tau};\tau) d_i. \tag{28}$$

When $\hat{\tau} \approx \tau$, the value of $\Lambda_{\text{acq}}(\hat{\tau};\tau)$ is

$$\Lambda_{\text{acq}}(\hat{\tau};\tau) = \frac{1}{L\eta} \sum_{i=0}^{L-1} r_i(\hat{\tau};\tau) d_i \tag{29}$$

$$= \frac{1}{L\eta} \sum_{i=0}^{L-1} s_i(\hat{\tau}-\tau) d_i + \frac{1}{L\eta} \sum_{i=0}^{L-1} w_i(\hat{\tau}) d_i \tag{30}$$

$$= \frac{1}{L\eta} \sum_{i=0}^{L-1} d_i \int s(t-\tau)\bar{\varphi}_i(t-\hat{\tau})\,\mathrm{d}t + \frac{1}{L\eta} \sum_{i=0}^{L-1} w_i(\hat{\tau}) d_i \tag{31}$$

$$= \frac{1}{L\eta} \sum_{i=0}^{L-1} d_i \int \sum_{j=0}^{L-1} d_j \varphi_j(t-\tau) \times \bar{\varphi}_i(t-\hat{\tau})\,\mathrm{d}t + \frac{1}{L\eta} \sum_{i=0}^{L-1} w_i(\hat{\tau}) d_i \tag{32}$$

$$\approx \frac{1}{L\eta} \sum_{i=0}^{L-1} \eta d_i^2 + \frac{1}{L\eta} \sum_{i=0}^{L-1} w_i(\hat{\tau}) d_i$$

$$= E_b + \frac{1}{L\eta} \sum_{i=0}^{L-1} w_i(\hat{\tau}) d_i.$$

Thus, when $\hat{\tau} \approx \tau$, $\Lambda_{\text{acq}}(\hat{\tau};\tau)$ is a Gaussian distribution with mean E_b and variance $\eta_d \sigma^2 E_b / L\eta$. Because $\Lambda_{\text{acq}}(\hat{\tau};\tau)$ is an irregular function that has many sharp peaks near the optimal solution (see Fig. 2), we cannot simply take the derivative and use the gradient descent approach to locate the maximum value position. We now introduce a serial state search algorithm that finds the maximum value position of $\Lambda_{\text{acq}}(\hat{\tau};\tau)$. The algorithm can be similarly applied to frame-timing acquisition in a $1/f$ noise environment. This is demonstrated in Appendix A.

3.1. Serial search algorithm

We measure the mean acquisition time to search for a time sufficiently close to the beginning of a frame (data block). This is essentially an estimation problem, for which many solutions have been proposed [8]. When a log-likelihood function has many sharp peaks, such as a code acquisition function for code-division multiple access (CDMA), the location of its maximum value cannot be identified easily from its derivative by a gradient descent approach. A popular and simple acquisition method for this is the serial search algorithm [9,10].

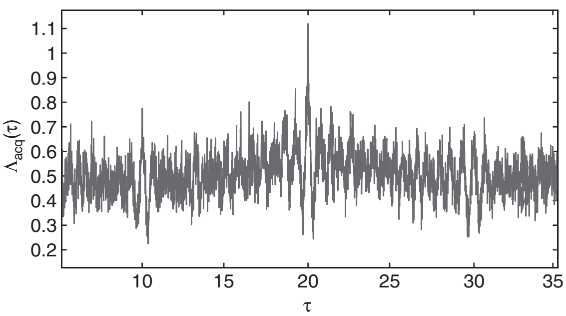

Fig. 2. An example of a bursty log-likelihood function. The parameters are $M = 3$, $L = 20$, $E_b/N_0 = 0$ dB, and $H = -1/2$. The unit in the vertical axis is E_b.

Fig. 3 shows a diagram of the serial search algorithm. There is a sequence of v points in the outer circle to be searched. The label in a branch denotes the probability that a transition occurs between points, multiplied by a power of z, where P_{D} and P_{F}, respectively, indicate the detection probability and the false alarm probability in testing whether the point is the correct timing. If the power of z is n, it indicates that $n\,\tau_{\mathrm{D}}$ seconds were required to make the transition. For a true hit, as with the branch labelled $P_{\mathrm{D}}z$, then the system has acquired the correct time and the search is complete. For a false alarm, the system takes τ_{D} seconds to move to an inner state. Afterwards, it takes $K\tau_{\mathrm{D}}$ seconds to verify the correctness of the detection and move from the inner state to the next outer state. A total of, a $(K+1)\tau_{\mathrm{D}}$ s are used to verify and move the system to the next point in the outer circle. This procedure is repeated until the correct time is acquired. The search time is the sum of the transition times of all the branches on the path in the diagram, under the assumption that any point is equally likely to be the initial point of the path.

The mean acquisition time for evaluating our acquisition algorithm is given below. Let us call the correct acquisition time point the destination point. Any branch in the inner circle moves to the next outer circle point with a delay of K. The transition from an outer circle point to the next outer circle point has the branch transfer function

$$H_b(z) = (1-P_{\mathrm{F}})z - P_{\mathrm{F}}z^{K+1}. \tag{35}$$

Then, the transfer function from an initial point that is i branches away from the destination point is

$$U_i(z) = \frac{H_b^i(z)P_{\mathrm{D}}z}{1-(1-P_{\mathrm{D}})zH_b^{v-1}(z)}. \tag{36}$$

Assume all points are, a priori, equally likely to be initial points, then the total transfer function average from all v starting points is

$$U(z) = \frac{1}{v}\sum_{i=0}^{v-1} U_i(z) = \frac{1}{v}\frac{P_{\mathrm{D}}z\sum_{i=0}^{v-1}H_b^i(z)}{1-(1-P_{\mathrm{D}})zH_b^{v-1}(z)} \tag{37}$$

$$= \frac{P_{\mathrm{D}}z[1-H_b^v(z)]}{v[1-H_b(z)][1-(1-P_{\mathrm{D}})zH_b^{v-1}(z)]}. \tag{38}$$

The mean acquisition time of a serial search algorithm, denoted as T_{acq}, is

$$T_{\mathrm{acq}} = \sum_{i=1}^{\infty} \mathrm{i}U_i = \left.\frac{\mathrm{d}U(z)}{\mathrm{d}z}\right|_{z=1}. \tag{39}$$

When $v \gg 1$, the mean acquisition time, in terms of P_{F} and P_{D}, is approximately

$$T_{\mathrm{acq}} \cong \frac{(2-P_{\mathrm{D}})(1+KP_{\mathrm{F}})}{2P_{\mathrm{D}}}(v\tau_{\mathrm{D}}). \tag{40}$$

The variance of the acquisition time is derived from the second derivative of $U(z)$ and is given as

$$\left.\left\{\frac{\mathrm{d}^2U(z)}{\mathrm{d}z^2} + \frac{\mathrm{d}U}{\mathrm{d}z}\left[1-\frac{\mathrm{d}U(z)}{\mathrm{d}z}\right]\right\}\right|_{z=1}. \tag{41}$$

When $v \gg 1$, in terms of P_{D} and P_{F}, the variance is written

$$\tau_{\mathrm{D}}^2\left\{(1+KP_{\mathrm{F}})^2v^2\left(\frac{1}{12}-\frac{1}{P_{\mathrm{D}}}+\frac{1}{P_{\mathrm{D}}^2}\right) + 6v[K(K+1)P_{\mathrm{F}}(2P_{\mathrm{D}}-P_{\mathrm{D}}^2) + (1+P_{\mathrm{F}}K)(4-2P_{\mathrm{D}}-P_{\mathrm{D}}^2)] + \frac{1-P_{\mathrm{D}}}{P_{\mathrm{D}}^2}\right\}. \tag{42}$$

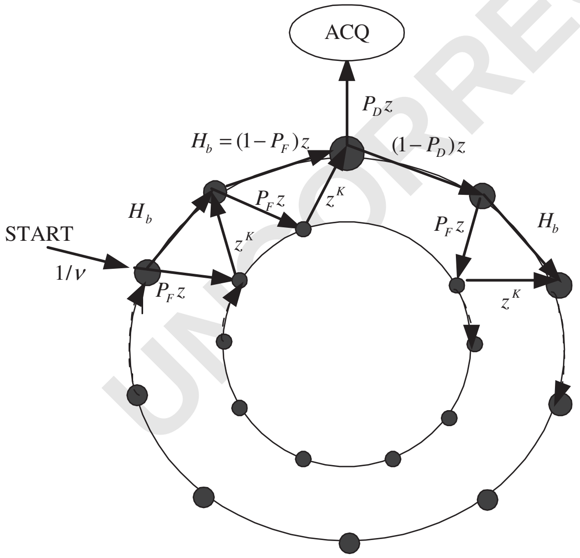

Fig. 3. A serial search state diagram. The points in the inner circle are false alarm states.

4. Simulation results

All the simulation programs are written in Matlab, and our wavelets $\psi_{m,n}(t)$ are approximated by discrete points. We use T_0 to denote the signaling interval (the time interval between two adjacent symbols) at the sub-band $m=0$, which is the bottom row in Fig. 1, and 128 points to represent the interval T_0. In all the experiments, we use the Meyer wavelet, which has a length of $16T_0$. The Meyer wavelet $\psi(t)$ has 2,048 discrete points in the slowest sub-band. Also, we choose $\beta=1$ for modulation. Because each symbol is either $\sqrt{E_b}$ or $-\sqrt{E_b}$, we use E_b/N_0 to denote the signal to noise ratio at each time-frequency cell. Note that, in an AWGN channel, all frequency cells have the same E_b/N_0.

The serial search algorithm parameters used here are selected as follows. Points in the outer circle are sampled at every half interval for each symbol in the sub-band with the shortest time interval per symbol. Thus, if we have M sub-bands and a data block with L symbols, then we will have $L2^{M-1}$ symbols in the sub-band $M-1$ in which the width of a symbol interval has the narrowest rectangular slot in the time domain, as in the top row of slots in Fig. 1. Hence, there are $v=L2^M$ points in the outer circle. The accuracy of our acquisition algorithm is within one-half a symbol interval at the sub-band $M-1$. The correct timing hypothesis is tested at any point in the outer circle by comparing $\Lambda_{\mathrm{acq}}(\tau)$ at the point to a given threshold. The hypothesis is accepted if the $\Lambda_{\mathrm{acq}}(\tau)$ is greater than the threshold. We determine our threshold value from the result of Eq. (34). Since $\Lambda_{\mathrm{acq}}(\hat{\tau};\tau)$ yields a mean value E_b when the timing is correctly acquired, our threshold T_h is set to be $0.7E_b$. Its value may not be the optimal threshold for minimizing the mean acquisition time. Determining the optimal threshold is an advanced topic that requires an analysis based on detection theory [11]. The detection probability P_{D} and the false alarm probability P_{F} (both of which are dependent on the threshold) used in estimating the mean acquisition time were obtained through simulations. K is the time required to realize that the current state is incorrect. Its value depends on the procedure to check the correctness of the current state.

We use the following procedure to verify the correctness of the current state. We assume that the detected start-of-frame point at $\hat{\tau}$ is the true start-of-frame. To verify the correctness of the assumption, we verify the K consecutive symbols by applying K fractal demodulations to the received signal at delay times $\hat{\tau}+iT_0/2^{M-1}$ with $i=1,2,\ldots,K$; N is the number of points to represent the wavelet $\psi(t)$ here, we have 2048 points). At the ith demodulation, we estimate the symbols in the time-frequency cells (there are η cells) that should contain the d_i symbol and compare each estimated symbol to d_i. If the estimated symbols in the cells are indeed d_i, we say that the symbol d_i is correctly received. If there are more than $\lfloor K/2\rfloor+1$ correctly received symbols, we say that the detected start-of-frame point is correct. In our experiment, we use $K=7$. This value is not necessarily the optimal value for our verification. Analysis of various verification processes and their performance are not within the scope of our study. Some verification methods for the CDMA serial search algorithm can be found in [12–14].

The top plot of Fig. 4 shows the received AWGN signal whose E_b/N_0 is 0 dB. The transmitted signal is a concatenation of three frames beginning at $\tau=40,60,80$. The bottom part shows the acquisition function. For the three data blocks in the signal, there are three peaks in the figure that occur at the correct timing points.

Fig. 5 shows the average detection probability P_{D}, the average false alarm probability P_{F}, and the mean acquisition time $T_{\mathrm{acq}}/\tau_{\mathrm{D}}$ versus E_b/N_0. For an E_b/N_0, the P_{D} and P_{F} are measured from 150 Monte-Carlo simulations of AWGN noisy signals. In the simulation, the parameters are $M=3$ and $L=20$. There are $L2^M=160$ outer states in our serial search algorithm. One of these is the destination state; the rest of the states are non-destination states. The detection probability P_{D} measures the average of the detected event (when $\Lambda_{\mathrm{acq}}(\hat{\tau};\tau)>T_h$) from all the simulated received signals and the destination state, while the false alarm probability P_{F} measures the average of the detected event from all realizations and all non-

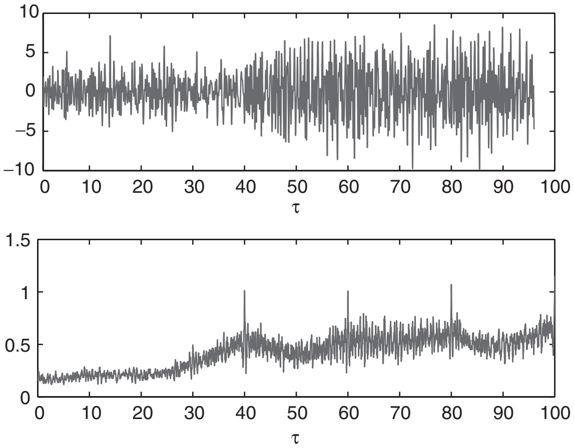

Fig. 4. Top: the received noisy signal. The transmitted self-similar signal (with $H = -\frac{1}{2}$) contains three data blocks; each block has 20 symbols. Bottom: the value of acquisition function. The unit of vertical axis is E_b. There are three peaks that occur every 20 τ.

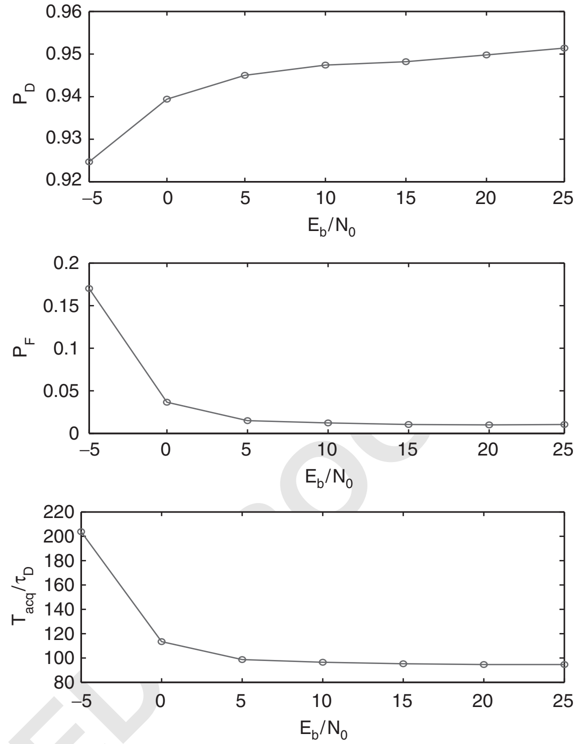

Fig. 5. Top: the detection probability. Middle: the false alarm probability. Bottom: the normalized mean acquisition time versus different E_b/N_0 in an AWGN channel. The experiment parameters are $L = 20$, $M = 3$, and $H = -\frac{1}{2}$. As shown in the figures, when E_b/N_0 increases, the false alarm probability P_F decreases and the detection probability P_D increases. According to Eq. (40), decreasing P_F and increasing P_D reduces the value of the denominator of the equation, thus, the mean acquisition decreases.

destination states. Our mean acquisition time is normalized against τ_D, which is the time consumed testing for the correct timing hypothesis at each outer circle point. When the false alarm probability is zero, the mean acquisition time is half the state number of our series search algorithm. In Fig. 5, as E_b/N_0 grows, the acquisition delay asymptotically is 80 τ_D, which is equal to half the state number in this experiment.

The effects of the block length L on P_D and P_F are shown in Fig. 6. According to Eq. (34), the noise variance decrease as the information vector L increases. Thus, P_D increases and P_F decreases as block length L increases. A longer buffer and time are needed at a receiver to collect and process a longer data vector. Since v is proportional to L, according to Eq. (40), the mean acquisition time is a linear function of L. This is shown in the bottom figure of Fig. 6.

5. Conclusion and future work

Because a technique to detect the start-of-frame of fractal modulation had yet to be developed, the diversity property of a fractal modulation could not be applied. Our frame timing acquisition algorithm uses a serial search algorithm to locate the beginning timing of all sub-bands in a delayed signal. The acquisition algorithm obtains the maximum-likelihood solution in AWGN channels. As our acquisition precision is proportional to the number of sampling points, by increasing the sampling rate, frame timing acquisition accuracy increases, but the acquisition time also increases. In the future, we plan to combine other synchronization techniques to obtain an efficient and accurate acquisition algorithm.

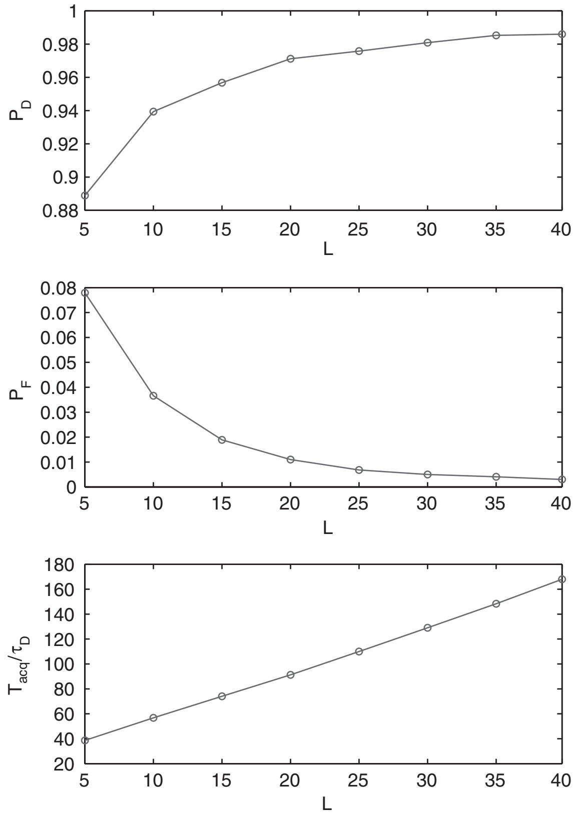

Fig. 6. Performance measurement against various data block lengths L in an AWGN channel. Top: the detection probability. Middle: the false alarm probability. Bottom: the mean acquisition time. Experiment parameters are $M = 3, E_b/N_0 = 0\,\mathrm{dB}$, and $H = -\frac{1}{2}$.

Acknowledgements

We would like to express our gratitude to the Reviewers for many insightful suggestions.

Appendix A. Spectrum matching—timing acquisition in a $1/f$ noise

The spectrum matching rule that maintains the same *SNR* across all frequencies leads to a uniform performance for a receiver operating with varying bandwidth [15,16]. This rule is potentially well-suited for transmitting fractal modulated signals where a receiver is operating in a channel with an unknown bandwidth. Here, we discuss fractal modulation and demodulation of a noisy signal that is embedded in a $1/f$ noise.

We assume that noise $w(t)$ in Eq. (15) is a Gaussian $1/f$ process whose degree $H_w = H$ has been estimated [17,18], and that the degree H_s of the signal $s(t)$ has been chosen to make it match the transmitted noise. Then, we have

$$H_s = H_w = H. \tag{43}$$

It was shown in [19] that an orthogonal wavelet is an almost whitening filter of any $1/f$ process. Furthermore, the wavelet coefficients of a Gaussian $1/f$ process can be well approximated as independent zero-mean Gaussian random variables with a variance depending on the scale and the fractal parameter H. That is,

$$w_{m,n}(\hat{\tau}) = \int w(t)\psi_{m,n}(t - \hat{\tau})\,\mathrm{d}t \tag{44}$$

and

$$E[w_{m,n}(\hat{\tau})w_{k,l}(\hat{\tau})] \approx \sigma^2\beta^{-m}\delta_{m,k}\delta_{n,l}. \tag{45}$$

The derivation of the above equation can be found in [19]. According to Eq. (11), we have

$$\begin{aligned} w_i(\hat{\tau}) &= \int w(t)\bar{\varphi}_i(t - \hat{\tau})\,\mathrm{d}t & (46)\\ &= \int w(t) \sum_{(m,n)\in G_i} \beta^{m/2}\psi_{m,n}(t - \hat{\tau})\,\mathrm{d}t & (47)\\ &= \sum_{(m,n)\in G_i} \int w(t)\beta^{m/2}\psi_{m,n}(t - \hat{\tau})\,\mathrm{d}t & (48)\\ &= \sum_{(m,n)\in G_i} \beta^{m/2} w_{m,n}(\hat{\tau}), & (49) \end{aligned}$$

where from Eq. (48)–(49) due to Eq. (44). Using the spectrum matching rule to decompose the $1/f$ process $w(t)$ by fractal basis $\bar{\varphi}_i(t - \hat{\tau})$, we obtain

$$E[w_i(\hat{\tau})] = \int E[w(t)]\bar{\varphi}_i(t - \hat{\tau})\,\mathrm{d}t = 0, \tag{50}$$

$$E[w_i(\hat{\tau})w_k(\hat{\tau})] = \sum_{(m,n)\in G_i} \sum_{(j,l)\in G_k} \beta^{m/2}\beta^{m/2} E[w_{m,n}(\hat{\tau})w_{j,l}(\hat{\tau})] \quad (51)$$

$$= \sum_{(m,n)\in G_i} \sum_{(j,l)\in G_k} \sigma^2 \delta_{m,j}\delta_{n,l} \quad (52)$$

$$= \sigma^2 \eta \delta_{i,k}. \quad (53)$$

The pdf of $\mathbf{r}$ for the spectrum matching method is derived by a similar method to that of Eq. (24), so we obtain

$$p(\mathbf{r}|\hat{\tau}-\tau,\mathbf{d}) = \left(\frac{1}{\sqrt{2\pi\eta}\sigma}\right)^L \exp\left\{-\frac{1}{2\eta\sigma^2} \times \sum_{i=0}^{L-1}[r_i(\hat{\tau};\tau) - s_i(\hat{\tau}-\tau)]^2\right\}. \quad (54)$$

We can use the same log-likelihood equation for AWGN (see Eq. (28)) for frame timing acquisition in an $1/f$ noise.

References

[1] G. Wornell, A.V. Oppenheim, Wavelet based representations for a class of self similar signals with applications to fractal modulation, IEEE Trans. Inform. Theory 38 (March 1992) 758–800.

[2] G. Wornell, Emerging applications of multirate signal processing and wavelets in digital communications, Proc. IEEE 84 (Apirl 1996) 586–603.

[3] L. Atzori, D.D. Giusto, M. Murroni, Performance analysis of fractal modulation transmission over fast-fading wireless channels, IEEE Trans. Broadcasting 48 (June 2002) 103–110.

[4] A.E. Bell, M. Manglani, Wavelet modulation in Rayleigh fading channels: improved performance and channel identification, in: Proceedings of IEEE ICASSP'02, vol. 3, Orlando, Florida, May 2002, pp. 2813–2816.

[5] S. He, Z. He, Blind equalization of nonlinear communication channels using recurrent wavelet neural networks, in: Proceedings of IEEE ICASSP'97, vol. 4, Munich, Germany, April, pp. 3305–3308.

[6] M. Luise, M. Marselli, R. Reggiannini, Clock synchronization for wavelet-based multirate transmissions, IEEE Trans. Commun. 48 (June 2000) 1047–1054.

[7] C.M. Fu, W.L. Hwang, C.L. Huang, Timing acquisition for wavelet-based multirate transmissions, in: Proceedings of IEEE GLOBECOM'03, vol. 4, San Francisco, USA, December 2003, pp. 2208–2212.

[8] K.H. Mueller, M. Muller, Timing recovery in digital synchronous data receivers, IEEE Trans. Commun. 24 (May 1976) 516–531.

[9] A. Polydoros, M.K. Simon, Generalized serial search code acquisition: the equivalent circular state diagram approach, IEEE Trans. Commun. 32 (1984) 1260–1268.

[10] A.J. Viterbi, Principles of Spread Spectrum Communication, Addison-Wesley Press, Reading, MA, 1995.

[11] H.V. Poor, An Introduction to Signal Detection and Estimation, Springer, Berlin, 1994.

[12] L.L. Yang, L. Hanzo, Serial acquisition of DS-CDMA signals in multipath fading mobile channels, IEEE Trans. Vehicular Technol. 50 (March 2001) 617–628.

[13] A. Polydoros, C. Weber, A unified approach to serial search spread-spectrum code acquisition–part I: general theory, IEEE Trans. Commun. 32 (May 1984) 542–549.

[14] A. Polydoros, C. Weber, A unified approach to serial search spread-spectrum code acquisition–part II: a matched-filter receiver, IEEE Trans. Commun. 32 (May 1984) 550–560.

[15] J.G. Proakis, Digital Communications, McGraw-Hill, New York, 1995.

[16] W.C. Lindsey, M.K. Simon, Telecommunication Systems Engineering, Prentice-Hall, Englewood Cliffs, NJ, 1973.

[17] G. Wornell, A.V. Oppenheim, Estimation of fractal signals from noisy measurements using wavelets, IEEE Trans. Signal Process. 38 (March 1992) 611–623.

[18] W.L. Hwang, Estimation of fractional Brownian motion embedded in a noisy environment using nonorthogonal wavelets, IEEE Trans. Signal Process. 47 (August 1998) 2211–2219.

[19] G. Wornell, A karhunen-loeve expansion for 1/f processes via wavelets, IEEE Trans. Inform. Theory 36 (July 1990) 859–861.